Title

Genetic and transcriptomic dissection of nitrate-independent function of Arabidopsis NRT1.1/NPF6.3/CHL1 under high ammonium condition

Authors and addresses

Takushi Hachiya[a,b,†], Nobue Makita[b], Liên Bach[c], Alain Gojon[c], Tsuyoshi Nakagawa[a], and Hitoshi Sakakibara[b,d]

[a]Department of Molecular and Functional Genomics, Interdisciplinary Center for Science Research, Shimane University, Matsue 690-8504, Japan

[b]RIKEN Center for Sustainable Resource Science, Tsurumi, Yokohama 230-0045, Japan

[c]Institut des Sciences des Plantes de Montpellier (IPSiM), Université de Montpellier, Centre National de la Recherche Scientifique (CNRS), Institut National de Recherche pour l'Agriculture, l'Alimentation, et l'Environnement (INRAE), Institut Agro, Montpellier, France

[d]Graduate School of Bioagricultural Sciences, Nagoya University, Nagoya 464-8601, Japan

Corresponding Author

Takushi Hachiya

Department of Molecular and Functional Genomics, Interdisciplinary Center for Science Research, Shimane University, Matsue 690-8504, Japan

Email: takushi.hachiya@life.shimane-u.ac.jp,

Tel: +81-852-32-6288, FAX: +81-852-32-6109

Abstract

The Arabidopsis nitrate transceptor NRT1.1/NPF6.3/CHL1 regulates physiological responses to nitrate. Several studies have reported that *Arabidopsis* lacking NRT1.1 shows enhanced shoot growth under toxic levels of ammonium without nitrate, suggesting a nitrate-independent function for NRT1.1. To further investigate this nitrate-independent function and its impact on ammonium tolerance, we conducted genetic analysis, tissue-specific expression analysis, and transcriptome analysis using various NRT1.1-related lines. Transgenic plants expressing either nonphosphomimic or phosphomimic mutants of NRT1.1 exhibited similar ammonium tolerance to the wild-type. The *chl1-9* mutant, in which NRT1.1 with the P492L substitution is localized intracellularly rather than at the plasma membrane and fails to transport nitrate, showed significantly improved ammonium tolerance. Confocal imaging revealed that the NRT1.1-GFP signal was detected in the plasma membrane of various tissues, including cotyledon pavement cells, hypocotyl epidermal cells, mesophyll cells, and epidermis and cortex near root tips. In early seedlings, the absence of functional NRT1.1 altered the expression of genes associated with aliphatic glucosinolate biosynthesis, ethylene signaling, and low pH stress. Genes predicted to encode products localized to the extracellular space were enriched among those differentially expressed due to *NRT1.1* deficiency. Our data suggest that in the absence of nitrate, plasma membrane-targeted NRT1.1 reduces ammonium tolerance irrespective of its phosphorylation state with alterations of gene expression associated with stress and senescence.

Key words: *Arabidopsis thaliana,* ammonium toxicity, CHL1, NPF6.3, NRT1.1

45 **1. Introduction**

46 Land plants primarily rely on soil nitrate as their main nitrogen (N) source. Nitrate
47 serves not just as a substrate for N assimilation but also as a vital signaling molecule,
48 regulating genes related to nitrogen acquisition and root system development (Wang et
49 al. 2004; Okamoto et al. 2019). These nitrate responses require molecular components
50 to perceive nitrate and to drive nitrate-dependent signaling. The Arabidopsis nitrate
51 transporter NRT1.1/NPF6.3/CHL1 plays a crucial role as a nitrate sensor, orchestrating
52 various plant responses to nitrate supply (Remans et al. 2006; Ho et al. 2009; Bouguyon
53 et al. 2015). Downstream of NRT1.1, calcium ions serve as secondary messengers,
54 stimulating the expression of nitrate-responsive genes, including the major high-affinity
55 nitrate transport gene *NRT2.1* (Riveras et al. 2015). Recent findings indicate that the
56 subgroup III protein kinase CPK perceives calcium signals and phosphorylates the
57 transcription factor NLP7 (Liu et al. 2017), which directly binds intracellular nitrate,
58 regulating nitrate-dependent gene expression (Liu et al. 2022). Furthermore, NRT1.1
59 enhances the expression of the transcription factor *ANR1* and the *AFB3* auxin receptor
60 gene in roots, promoting lateral root development and elongation in response to nitrate
61 supply (Remans et al. 2006; Vidal et al. 2010). The magnitude of these
62 NRT1.1-dependent responses is finely tuned by the phosphorylation status of NRT1.1 at
63 the T101 residue (Ho et al. 2009; Bouguyon et al. 2015).

64 In addition to its nitrate-dependent functions, NRT1.1 exhibits significant roles in
65 the absence of nitrate. It aids the basipetal transport of auxin out of the lateral root
66 primordia when nitrate is absent (Krouk et al. 2010). Exogenous nitrate inhibits auxin

67 transport, leading to auxin accumulation in primordia and the stimulation of lateral root
68 emergence in nitrate-rich patches (Mounier et al. 2014). Walch-Liu and Forde (2008)
69 observed that exogenous glutamate inhibits primary root elongation at the root tip, a
70 process antagonized by nitrate presence, depending on phosphorylated NRT1.1.
71 Intriguingly, overexpression of nonphosphomimetic NRT1.1 (T101A) heightens
72 glutamate sensitivity in primary roots even without nitrate. Furthermore, studies
73 including ours have demonstrated that the absence of functional NRT1.1 significantly
74 alleviates growth suppression and chlorosis under toxic ammonium levels as the sole N
75 source (Hachiya et al. 2011; Jian et al. 2018; Liu et al. 2020). NRT1.1 promotes
76 ammonium accumulation, altering ammonium metabolism and subsequently
77 upregulating ethylene signaling, resulting in ammonium toxicity (Jian et al. 2018).
78 Moreover, under high ammonium and NaCl concentrations without nitrate, NRT1.1
79 transports chloride, leading to chloride accumulation, especially in roots (Liu et al.
80 2020). This chloride accumulation contributes to ammonium toxicity under high salt
81 conditions.

82 The aforementioned observations clearly indicate a nitrate-independent function for
83 NRT1.1, although the precise mechanism remains elusive. This study aimed to
84 comprehensively uncover the primary nitrate-independent function of NRT1.1 in
85 ammonium tolerance. Employing various NRT1.1-related lines, we conducted genetic
86 analyses, tissue-specific expression studies using quantitative PCR (qPCR) and confocal
87 microscopy, and transcriptome analyses. Our findings reveal that (i) plasma
88 membrane-targeted NRT1.1 diminishes ammonium tolerance regardless of its

89 phosphorylation state, (ii) NRT1.1 is expressed across most seedling tissues, and (iii)
90 NRT1.1 primarily modulates the expression of genes associated with aliphatic
91 glucosinolate (GSL) biosynthesis, ethylene signaling, and low pH stress.
92

93 **2. Materials and Methods**

94 ***2.1. Plant materials and growth conditions***

95 In this study, *A. thaliana* was used. The T-DNA insertion mutants *nrt1.1* (Hachiya et al.
96 2011), *cipk23-4* (Ho et al. 2009), and the gamma ray-mutagenized mutant c*hl1-5* (Tsay
97 et al. 1993a) in the Col background were obtained from the European Arabidopsis Stock
98 Center (NASC). The gamma-ray-mutagenized mutant *chl1-6* in the L*er* background
99 (Tsay et al. 1993b) was sourced from the Arabidopsis Biological Resource Center. The
100 transposon tag line *pst16286* in the Nossen background (Ito et al. 2002; Kuromori et al.
101 2004) was purchased from the RIKEN Bioresource Center (BRC). The lines harboring
102 the estradiol-inducible *NRT1.1-mCherry* and the *pNRT1.1:NRT1.1-GFPloop* in the
103 *chl1-5* background were used in previous studies (Bouguyon et al. 2015; Bouguyon et al.
104 2016). The *chl1-9* in the Col background and the *T101D* and *T101A* lines in the *chl1-5*
105 background (Ho et al. 2009) were provided by Dr. Yi-Fang Tsay (Academia Sinica).
106 The seeds underwent surface sterilization and were placed in plastic Petri dishes
107 (diameter: 90 mm; depth: 20 mm; Iwaki, Tokyo, Japan) with approximately 30 mL of
108 N-modified Murashige and Skoog medium. The medium included 4.7 mM MES-KOH
109 (pH 5.7), 2% (w/v) sucrose, and 0.25% (w/v) gellan gum (Wako, Osaka, Japan). Two
110 different N and K sources were used: 10 mM KNO_3 (10 mM NO_3^- condition) or 5 mM

111 $(NH_4)_2SO_4$ with 10 mM KCl (10 mM NH_4^+ condition). After being kept in the dark at
112 4 °C for 3 d, the plants were grown horizontally under a photosynthetic photon flux
113 density of 100–130 μmol m^{-2} s^{-1} (16 h light/8 h dark cycle) at 23 °C. For transfer
114 experiments, surface-sterilized seeds were sown in larger plastic Petri dishes (length:
115 140 mm; width: 100 mm; depth: 20 mm; Eiken Chemical Co. Ltd., Taito-ku, Tokyo,
116 Japan) containing 50 mL of half-strength modified Murashige and Skoog medium with
117 2.5 mM ammonium as the sole N source at pH 6.7 (Okamoto et al. 2019). After 3 days
118 in the dark at 4 °C, the plants were grown vertically for 5 d under a photosynthetic
119 photon flux density of 100–130 μmol m^{-2} s^{-1} (16 h light/8 h dark cycle) at 23 °C. The
120 plants were then transferred to different N conditions for subsequent experiments.
121 Further details regarding plantlet cultivation are provided in the Results section and
122 figure legends.

123 ***2.2. Extraction of RNA***

124 The seedlings were harvested and promptly frozen in liquid N_2, then stored at −80 °C
125 until needed. The frozen samples were ground using TissueLyser II (QIAGEN) with
126 zirconia beads (5 mm diameter). Total RNA was extracted using the RNeasy Plant Mini
127 Kit (Qiagen) and treated with on-column DNase digestion following the manufacturer's
128 instructions.

129 ***2.3. RT-qPCR***

130 Reverse transcription (RT) was conducted using ReverTra Ace qPCR RT Master Mix
131 with gDNA Remover (Toyobo Co. Ltd., Tokyo, Japan) following the manufacturer's
132 guidelines. The resulting cDNA was diluted tenfold with distilled water for quantitative

133 PCR (qPCR). Transcript levels were assessed using a StepOnePlus Real-Time PCR
134 System (Thermo Fisher Scientific, Waltham, MA, USA). In the presence of 10-μL
135 KAPA SYBR FAST qPCR Kit (Nippon Genetics Co. Ltd., Tokyo, Japan), 0.4 μL
136 specific primers (0.2 μM final concentration), and 7.2 μL sterile water, 2 μL of obtained
137 cDNA was amplified. *ACTIN3* (Hachiya et al. 2021) served as internal standards.
138 Standard curves were generated using plasmid DNA containing target cDNAs or total
139 cDNAs. Refer to Supplementary Table 1 for primer sequences.

140 ***2.4. Microarray analysis***

141 Microarray analysis was conducted following the protocol outlined in Hachiya et al.
142 (2021). RNA quality was evaluated using an Agilent 2100 bioanalyzer (Agilent
143 Technologies). RNA amplification, labeling, hybridization, and scanning were
144 performed using the 3′ IVT Express Kit (Affymetrix) and GeneChip Arabidopsis
145 Genome ATH1 Array (Affymetrix) as per the manufacturer's instructions. Data from
146 the microarray chips were normalized using the Microarray Suite 5.0 (MAS5) method
147 (Affymetrix). Transcripts labeled as "absent" or "marginal" were excluded from
148 subsequent quantitative analysis. The raw microarray data used in this study are
149 accessible in the ArrayExpress database at EMBL-EBI under accession number
150 E-MTAB-13395.

151 ***2.5. Observation of cotyledon***

152 Bright-field imaging of *Arabidopsis* early seedling cotyledons was conducted using an
153 all-in-one fluorescence microscope (BZ-X710, KEYENCE, Japan) equipped with a
154 Nikon 40× objective (CFI Plan Apo λ 40×/0.95). To create a high-resolution and

155 wide-area continuous image of the cotyledon, individual images were seamlessly
156 merged using the image joint function of the BZ analyzer software (KEYENCE).

157 ***2.6. Observation of fluorescent signal***

158 Confocal imaging of NRT1.1-GFPloop and propidium iodide (PI) was performed using
159 a Leica SP5 Confocal Microscope (Leica Microsystems). Roots were stained with a 10
160 μg mL^{-1} PI solution to outline cell shapes. Mesophyll protoplasts were prepared from
161 cotyledons of 12-day-old plants (3 days post-transfer from 9-day-old plants grown
162 under 10 mM nitrate) following the method of Endo et al. (2016). NRT1.1-GFPLoop
163 and PI were excited with 488 nm and 543 nm lasers, and emissions were detected from
164 500 to 530 nm and 590 to 660 nm, respectively, using a Leica 25× objective (HCX
165 IRAPO L 25×/0.95 WATER).

166 ***2.7. Statistical analysis***

167 The unpaired two-tailed Welch's *t*-test and the Tukey–Kramer multiple comparison test
168 were conducted using R software v.2.15.3. Additionally, the two-tailed ratio paired
169 t-test was performed using GraphPad Prism software v.9.3.1, assuming a Gaussian
170 distribution.

171

172 **3. Results**

173 ***3.1. NRT1.1 targeted to the plasma membrane reduces ammonium tolerance almost***
174 ***regardless of its phosphorylation status***

175 In our previous study, *NRT1.1*-deficient mutants in the Col background exhibited
176 enhanced shoot growth under 10 mM ammonium conditions (Hachiya et al. 2011). In

177 this study, we consistently observed larger shoot fresh weights (FWs) in
178 *NRT1.1*-deficient mutants from three Arabidopsis accessions (Col; *chl1-5*, *nrt1.1*, *Ler*;
179 *chl1-6*, and Nossen; *pst16286*) compared to wild-type plants under 10 mM ammonium.
180 Conversely, under 10 mM nitrate conditions, the FWs were lower in these mutants
181 (Figure 1a, b). Intriguingly, the induction of NRT1.1-mCherry in the *chl1-5* background,
182 controlled by β-estradiol (Bouguyon et al. 2015), significantly reduced shoot FW under
183 ammonium, whereas β-estradiol-treated Col plants did not show a change in FW
184 (Figure 1c). Under nitrate, shoot growth was restored by the induction of
185 NRT1.1-mCherry, confirming its functionality (Figure 1d). These findings underscore
186 the significant role of Arabidopsis NRT1.1 in ammonium tolerance.

187 NRT1.1 exhibits diverse molecular functions, including nitrate uptake, nitrate
188 sensing/signaling, and auxin transport (Ho et al. 2009; Krouk et al. 2010; Bouguyon et
189 al. 2015; Zhang et al. 2019). Modifications at specific residues in the protein alter these
190 functions. In the *chl1-9* mutant with the P492L substitution, NRT1.1 primarily localizes
191 inside the cell, impairing nitrate and auxin transport without affecting *NRT2.1* induction
192 by nitrate (Ho et al. 2009; Bouguyon et al. 2015). Transgenic plants expressing
193 nonphosphomimic (T101A) or phosphomimic (T101D) mutants of NRT1.1 show
194 distinct nitrate-dependent responses and auxin transport abilities. When grown on 10
195 mM ammonium, the *chl1-9* mutant exhibited markedly improved ammonium tolerance
196 compared to the wild-type, displaying larger FWs and higher chlorophyll concentrations
197 (Figure 1e–g). Except for slightly enhanced shoot growth in T101A compared to Col,
198 both T101 mutants displayed ammonium toxicity similar to Col. Moreover, *cipk23-4*,

199 lacking CIPK23 that phosphorylates NRT1.1 at the T101 residue (Ho et al. 2009), did
200 not exhibit enhanced shoot growth under ammonium or nitrate conditions (Figure 1h, i).
201 These results imply that NRT1.1-induced ammonium toxicity is nearly independent of
202 its phosphorylation at the T101 residue but requires correct plasma membrane targeting
203 dependent on the P492 residue.

204 To determine the developmental stages at which NRT1.1 affects ammonium
205 tolerance, we monitored the growth progression of Col and *chl1-5* plants under 10 mM
206 ammonium. In 3-day-old seedlings, there were no significant difference in FW, and
207 their appearances were similar (Figure 1j, l). By day 5, *chl1-5* seedlings exhibited larger
208 shoot and root FWs, and their cotyledons were more expanded and greener compared to
209 Col (Figure 1k, l, and S1a). Additionally, at this stage, *chl1-5* and *nrt1.1* seedlings had
210 significantly higher chlorophyll concentrations than Col (Figure S1b). As plants aged
211 between 8 and 11-days, the impact of *NRT1.1* deficiency on shoot growth intensified
212 compared to root growth (Figure 1k). These findings highlight that NRT1.1's influence
213 on ammonium tolerance initiates at the early stages of seedling growth.

214 ***3.2. A significant expression of NRT1.1 is detectable both in shoots and roots of***
215 ***ammonium-grown seedlings***

216 To decipher how NRT1.1 impacts ammonium tolerance, we examined *NRT1.1*
217 expression patterns in Col plants grown under 10 mM ammonium or 10 mM nitrate. In
218 3-day-old Col seedlings, *NRT1.1* expression showed little disparity between ammonium
219 and nitrate conditions (Figure 2a). However, in 5-, 8-, and 11-day-old plants, shoot
220 expression of *NRT1.1* remained consistently higher under 10 mM ammonium compared

221 to 10 mM nitrate, whereas in the roots, this trend reversed (Figure 2b). Consequently,
222 the disparity in *NRT1.1* transcript levels between shoot and root was smaller under
223 ammonium than nitrate. Furthermore, to investigate NRT1.1 protein expression under
224 ammonium conditions, we utilized the *pNRT1.1:NRT1.1-GFPloop* line for confocal
225 observation (Bouguyon et al. 2016). Clear GFP signals were localized in the plasma
226 membrane of various cells, including pavement cells of cotyledons (Figure 2c, i),
227 epidermal cells of hypocotyl (Figure 2d), mesophyll protoplasts (Figure 2e), and
228 epidermal and cortex cells of the primary root (Figure 2f, g). Intriguingly, dotted GFP
229 signals were frequently detected in intracellular regions of pavement cells and root tips
230 (Figure 2h, j). These expression analyses indicate that NRT1.1 might function in diverse
231 cells and tissues under high ammonium conditions.

232 ***3.3. Overview of genome-wide transcriptional responses caused by NRT1.1 deficiency***

233 To unravel the primary mechanisms by which NRT1.1 controls genome-wide gene
234 expression under ammonium conditions, we conducted independent microarray
235 experiments using 3-day-old (72 h) and 5-day-old (120 h) seedlings of Col, *chl1-5*, and
236 *nrt1.1*. In 3- and 5-day-old seedlings, we identified 20 and 176 transcripts, respectively,
237 in which expression was at least two-fold higher in both *NRT1.1*-deficient mutants
238 compared to Col (Table S2). Conversely, 13 and 80 transcripts in the mutants exhibited
239 levels less than or equal to half of those in Col (Table S2). To capture more
240 NRT1.1-regulated genes in the 3-day-old seedlings, we re-explored differentially
241 expressed genes (DEG) at a 1.5-fold threshold. This analysis identified 120 upregulated
242 genes and 71 downregulated genes in the mutants relative to Col (Table S3). RT-qPCR

243 analysis of 12 DEGs confirmed that the results were consistent with those of the
244 microarray (Figure S2 and Tables S2, 3). For subsequent analyses, we concentrated on
245 DEGs at a 1.5-fold threshold for 3-day-old seedlings and a 2-fold threshold for
246 5-day-old seedlings. A Venn diagram revealed that only 26 DEGs were common to both
247 3-day-old and 5-day-old seedlings (Figure 3a and Table S4). Enrichment analysis
248 conducted using Metascape (Zhou et al. 2019) identified a significant enrichment of the
249 term "response to extracellular stimulus" (Figure S3a). Additionally, the SUBA
250 localization predictor (Hooper et al. 2017) indicated that the translational products
251 corresponding to 9 out of the 26 DEGs were likely localized in the extracellular space
252 (Figure S3b). These findings suggest that, under ammonium conditions, NRT1.1 could
253 influence extracellular events.

254 In 3-day-old seedlings, the absence of NRT1.1 led to significant gene expression
255 changes without altering seedling growth (Figure 1e, 3a). Thus, we focused on the
256 transcriptome profile of 3-day-old seedlings to uncover the primary functions of
257 NRT1.1 under ammonium conditions. Gene cloud analysis (Krouk et al. 2015) revealed
258 a 168-fold enrichment in "methionine-derived" and a 120-fold enrichment in
259 "4-reductase" genes in the upregulated genes of 3-day-old *NRT1.1*-deficient mutants
260 (Figure 3b). "Methionine-derived" genes included *At3g19710* (*BCAT4*), *At4g12030*
261 (*BAT5*), and *At5g23010* (*MAM1*), essential for aliphatic glucosinolate biosynthesis. The
262 "4-reductase" genes included *At2g47460* (*MYB12*), *At4g09820* (*bHLH042*), and
263 *At5g42800* (*DFR*), contributing to flavonoid biosynthesis. Metascape analysis also
264 overrepresented terms like "glucosinolate biosynthesis from methionine" and

265 “flavonoid metabolic process” for upregulated genes in the mutants (Figure 3c).
266 Downregulated genes in the 3-day-old mutants enriched terms like “interpro-ipr008263
267 (glycoside hydrolase, family 16, active site)” from genes encoding cell wall-modifying
268 enzymes like xyloglucan endotransglucosylase/hydrolase (*At4g25810* (*XTH23*),
269 *At4g14130* (*XTH15*), and *At5g57560* (*XTH22*)) (Figure 3b). Intriguingly, DEGs in the
270 3-day-old mutants often overrepresented terms related to the extracellular space, such as
271 “plant-type cell wall loosening,” “secretory vesicle,” “apoplast,” “xyloglucan metabolic
272 process,” “plant-type cell wall,” and “xyloglucan:xyloglucosyl transferase activity”
273 (Figure 3c, d).

274 In 5-day-old seedlings, terms related to photosynthesis were predominant among
275 upregulated genes in response to *NRT1.1* deficiency (Figure S4a, b). This aligns with
276 the observed greener and more expanded cotyledons and higher chlorophyll
277 concentrations in *NRT1.1*-deficient seedlings compared to Col (Figure 1m and S1a, b).
278 Conversely, downregulated genes were associated with terms related to abiotic and
279 biotic stresses (Figure S4c). MapMan analysis clearly illustrated the upregulation of
280 genes encoding components for light reactions, chlorophyll biosynthesis, and the
281 Calvin–Benson cycle in 5-day-old *NRT1.1*-deficient mutants (Figure S5b). These
282 findings indicate an enhancement of photoautotrophic growth with reduced stress
283 response in the 5-day-old mutants.

284 ***3.4. Effects of NRT1.1 deficiency on expression of genes for glucosinolate***
285 ***biosynthesis and genes responsive to ACC, NaCl, H_2O_2, IAA, and low pH under***
286 ***ammonium condition***

287 Initially, we concentrated on the genes involved in the biosynthesis of aliphatic GSL
288 and indole GSL, based on the gene list from Harun et al. (2020). This focus was due to
289 the enrichment of terms such as "glucosinolate biosynthesis from methionine,"
290 "methionine-derived," and "glucosinolate biosynthesis" among the upregulated genes in
291 3- and 5-day-old *NRT1.1*-deficient mutants (Figures 3b, c, and S5b). The deficiency of
292 *NRT1.1* significantly upregulated the aliphatic GSL biosynthesis genes and their
293 positive regulator genes, *AT5G61420* (*MYB28*) and *AT5G07690* (*MYB29*), while it had
294 little effect on the expression of indole GSL biosynthesis genes (Figure 4a and Tables
295 S2, 3, and 5).

296 Our enrichment analysis revealed that the GO term "cellular response to ethylene
297 stimulus" was overrepresented among the downregulated genes in 3-day-old
298 *NRT1.1*-deficient mutants (Figure 3d). This aligns with a previous study that reported a
299 down-regulation of genes involved in ethylene biosynthesis and senescence under toxic
300 ammonium conditions in *NRT1.1*-deficient mutants (Jian et al. 2018). Consequently, we
301 examined the genes responsive to the application of 1-aminocyclopropane-1-carboxylic
302 acid (ACC), a precursor of ethylene whose biosynthesis is a rate-limiting step for
303 ethylene production, based on the gene list from Goda et al. (2008) (Figure 4b and
304 Table S6). The ACC-induced genes were significantly downregulated in both 3- and
305 5-day-old *NRT1.1*-deficient mutants grown under 10 mM ammonium, whereas the
306 ACC-repressed genes did not show a significant response.

307 The GO term "response to salt stress" was found to be overrepresented in the
308 downregulated genes of 3- and 5-day-old *NRT1.1*-deficient mutants (Figures 3d and

309 S4c). A recent study found that in the presence of a 25 mM chloride ion with
310 ammonium as the sole N source, NRT1.1 supports excessive chloride absorption,
311 resulting in severe root growth inhibition (Liu et al. 2020). *NRT1.1* deficiency may
312 affect the expression of NaCl-responsive genes because our ammonium solution
313 contains 16 mM chloride ions. The NaCl-induced genes listed from Shen et al. (2014)
314 were significantly downregulated in the 5-day-old *NRT1.1*-deficient mutants, but not in
315 the 3-day-old mutants (Figures 4c and Table S7). The expression of NaCl-repressed
316 genes differed little between Col and *NRT1.1*-deficient mutants.

317 It has been reported that ammonium nutrition disrupts redox homeostasis, leading
318 to the apoplastic accumulation of reactive oxygen species and oxidative stress
319 (Podgórska et al. 2015). In line with this, our enrichment analysis revealed the presence
320 of the GO terms "response to oxidative stress" and "antioxidant activity" among the
321 downregulated genes in both 3-day-old and 5-day-old *NRT1.1*-deficient mutants (Figure
322 3d and S4c). Genes that are upregulated in response to H_2O_2 application, as documented
323 by Hieno et al. (2019), were downregulated in the 5-day-old *NRT1.1*-deficient mutants,
324 but not in the 3-day-old mutants (Figure 4d and Table S8). No significant alterations in
325 the expression of genes downregulated by H_2O_2 were observed between Col and the
326 *NRT1.1*-deficient mutants.

327 Regarding auxin responses, although NRT1.1 facilitates auxin influx into the cell
328 in the absence of nitrate (Krouk et al. 2010), its deficiency did not significantly alter the
329 expression of typical genes responsive to indole-3-acetic acid (IAA) application (Goda
330 et al. 2008) (Figure 4e and Table S9).

331 Interestingly, previous studies have shown that 43% of ammonium-inducible genes
332 correspond to low pH (4.5)-inducible genes in *A. thaliana* (Lager et al. 2010; Patterson
333 et al. 2010). We have previously observed that the enhanced ammonium tolerance of
334 *NRT1.1*-deficient mutants at pH 5.7 was mimicked in Col plants grown at pH 6.7
335 (Hachiya et al. 2011). These findings suggest that *NRT1.1*-deficient mutants may
336 exhibit enhanced tolerance to ammonium-derived acidic stress. Consequently, we
337 examined the microarray data with a focus on low pH stress-responsive genes listed in
338 Lager et al. (2010). Remarkably, the low pH stress-inducible genes were significantly
339 downregulated both in the 3- and 5-day-old *NRT1.1*-deficient mutants relative to Col,
340 whereas the low pH stress-repressive genes were generally upregulated in the mutants
341 (Figure 4f and Table S10).
342 Collectively, we conclude that NRT1.1 primarily alters the expression of genes
343 associated with aliphatic glucosinolate biosynthesis, ethylene signaling, and low pH
344 stress.
345
346 **4. Discussion**
347 The Arabidopsis nitrate transceptor NRT1.1 and its orthologs are required for plant
348 adaptation to nitrate-rich conditions (Wang et al. 2020). NRT1.1, on the other hand, has
349 been shown to reduce ammonium tolerance in the absence of nitrate (Hachiya et al.
350 2011; Jian et al. 2018). Thus, NRT1.1 and its orthologs are likely to determine adaption
351 features for the two major N sources, nitrate and ammonium.

352 Excessive ammonium assimilation by plastidic glutamine synthetase produces
353 proton accumulation and acidic stress in *A. thaliana* shoots when exposed to high
354 amounts of ammonium (Hachiya et al. 2021). Proton excretion from plants to external
355 media is common in plant cultivation with high ammonium feeding (Britto and
356 Kronzucker 2002). Moreover, in *A. thaliana*, ammonium-inducible genes and low pH
357 (4.5)-inducible genes overlap at a significant rate (Lager et al. 2010, Patterson et al.
358 2010). These findings imply that acidic stress is a major source of ammonium toxicity.
359 Our transcriptome analysis revealed that *NRT1.1* deficiency dampens low pH responses
360 (Figure 4f). We observed that increasing the pH of the medium from 5.7 to 6.7 by
361 adding alkaline NH_3 solution promoted shoot development of Col more intensely than
362 that of *chl1-5* under ammonium conditions, virtually completely suppressing the
363 difference in growth (Figure S6). These suggest that NRT1.1 exacerbates acidic stress
364 in the presence of ammonium. Interestingly, an acidic rhizosphere induces *NRT1.1*
365 expression in a STOP1 transcription factor-dependent way, which enhances symport of
366 proton and nitrate through NRT1.1 and adjusts rhizosphere pH to a more suitable range
367 (Ye et al. 2021). Furthermore, NRT1.1 and SLAH3 collaborate to drive a nitrate cycle
368 across the plasma membrane, reducing acidification of the rhizosphere (Xiao et al.
369 2022). It is uncertain how NRT1.1 affects intra- and extracellular pH under nitrate-free
370 ammonium conditions.

371 Our transcriptome analysis highlighted the extracellular space as an early site of
372 NRT1.1 action (Figure 3c, d, and S3a, b, S4b, c). A study by Podgórska et al. (2017) in
373 *A. thaliana* demonstrated that ammonium toxicity is associated with smaller mesophyll

374 cells characterized by a more rigid cell wall structure, containing increased phenolic
375 compounds and boron ions. In our study, the GO terms "plant-type cell wall loosening"
376 and "plant-type cell wall modification" were enriched in the genes upregulated by
377 *NRT1.1* deficiency (Figure 3c and S4b). These terms originated from genes encoding
378 proteins involved in cell wall loosening and cell expansion, such as *AT1G69530*
379 (*EXPA1*), *AT1G74670* (*GASA6*), *AT2G20750* (*EXPB1*), *AT2G40610* (*EXPA8*),
380 *AT3G29030* (*EXPA5*), and *AT4G28250* (*EXPB3*). This suggests that NRT1.1 might
381 influence ammonium tolerance via alterations in cell wall modification processes.

382 We discovered that genes for aliphatic GSL biosynthesis and their positive
383 regulator genes, *MYB28* and *MYB29*, were induced by *NRT1.1* deficiency (Figure 4a,
384 S2b, Table S2, 4). Coleto et al. (2021) reported that ammonium toxicity was
385 exacerbated in the *myb28myb29* mutant but not in the *myc234* mutant. Given that both
386 mutants are almost devoid of aliphatic GSL, the ammonium hypersensitivity of
387 *myb28myb29* is not linked with a lack of aliphatic GSL. The authors provided evidence
388 that MYB28 and MYB29 maintain intracellular iron homeostasis under ammonium
389 conditions, thereby attenuating ammonium toxicity. It remains to be seen whether the
390 absence of NRT1.1 enhances ammonium tolerance via upregulation of *MYB28* and
391 *MYB29*. Meanwhile, our transcriptome data suggested that NRT1.1 enhances ethylene
392 signaling under ammonium conditions. Plants emit ethylene as a phytohormone in
393 response to various stresses, including ammonium toxicity (Britto and Kronzucker
394 2002). Inhibition of ethylene signaling by gene knockout and chemical treatment
395 alleviates ammonium toxicity (Jian et al. 2018, Li et al. 2019). These findings suggest

396 that NRT1.1 reduces ammonium tolerance through ethylene signaling. Although there is
397 little overlap among aliphatic GSL biosynthesis genes and ACC- and low
398 pH-responsive genes (Tables S5, 6, 10), it would be worthwhile to scrutinize these
399 associations.
400

401 **Acknowledgments**
402 We are grateful for Dr. Carine Alcon and Montpellier RIO Imaging on technical support
403 with confocal microscopy. We would like to thank Dr. Yi-Fang Tsay (Academia Sinica)
404 for giving the Arabidopsis seeds. We would also like to thank Enago (www.enago.jp)
405 for the English language review.
406

407 **Disclosure statement**
408 The authors report there are no competing interests to declare.
409

410 **Funding**
411 This study was supported by the Grants-in-Aid from the Ministry of Education, Culture,
412 Sports, Science and Technology, Japan (No. 17K15237, JP20K05771, JP23K04978 to
413 TH), by the Inamori Foundation (to TH), by the Agropolis Foundation (No. 1502-405 to
414 TH), and by the Nagase Science and Technology Foundation (to TH).
415
416
417

418 **References**

419 Bouguyon, E., F. Brun, D. Meynard, M. Kubeš, M. Pervent, S. Leran, B. Lacombe et al. 2015.
420 “Multiple mechanisms of nitrate sensing by Arabidopsis nitrate transceptor NRT1.1.” Nature
421 Plants 1: 15015. doi:10.1038/nplants.2015.15.
422
423 Bouguyon, E., F. Perrine-Walker, M. Pervent, J. Rochette, C. Cuesta, E. Benkova, A.
424 Martinière, L. Bach, G. Krouk, A. Gojon, and P. Nacry. 2016. "Nitrate controls root
425 development through posttranscriptional regulation of the NRT1.1/NPF6.3 transporter/sensor."
426 Plant Physiology 172: 1237-1248. doi:10.1104/pp.16.01047.
427
428 Britto, D. T., and H. J. Kronzucker. 2002. "NH_4^+ toxicity in higher plants: a critical review."
429 Journal of Plant Physiology 159(6): 567-584. doi:10.1078/0176-1617-0774.
430
431 Coleto, I., I. Bejarano, A. J. Marín-Peña, J. Medina, C. Rioja, M. Burow, and D. Marino. 2021.
432 "*Arabidopsis thaliana* transcription factors *MYB28* and *MYB29* shape ammonium stress
433 responses by regulating Fe homeostasis." New Phytologist 229(2): 1021-1035.
434 doi:10.1111/nph.16918.
435
436 Goda, H., E. Sasaki, K. Akiyama, A. Maruyama-Nakashita, K. Nakabayashi, W. Li, M. Ogawa,
437 Y. Yamauchi, J. Preston, K. Aoki et al. "The AtGenExpress hormone and chemical treatment
438 data set: experimental design, data evaluation, model data analysis and data access." The Plant
439 Journal 55(3): 526-542. https://doi.org/10.1111/j.1365-313X.2008.03510.x.

Hachiya, T., Y. Mizokami, K. Mizokami, D. Tholen, C. K. Watanabe, and K. Noguchi. 2011. "Evidence for a nitrate-independent function of the nitrate sensor NRT1.1 in *Arabidopsis thaliana*." Journal of Plant Research 124: 425-430. doi:10.1007/s10265-010-0385-7.

Hachiya, T., J. Inaba, M. Wakazaki, M. Sato, K. Toyooka, A. Miyagi, M. Kawai-Yamada, D. Sugiura, T. Nakagawa, T. Kiba, A. Gojon, and H. Sakakibara. 2021. "Excessive ammonium assimilation by plastidic glutamine synthetase causes ammonium toxicity in *Arabidopsis thaliana*." Nature Communications 12(1): 4944. doi:10.1038/s41467-021-25238-7.

Harun, S., M. R. Abdullah-Zawawi, H. H. Goh, and Z. A. Mohamed-Hussein. 2020. "A comprehensive gene inventory for glucosinolate biosynthetic pathway in *Arabidopsis thaliana*." Journal of agricultural and food chemistry 68(28): 7281-7297. doi:10.1021/acs.jafc.0c01916.

Hieno, A., H. A. Naznin, K. Inaba-Hasegawa, T. Yokogawa, N. Hayami, M. Nomoto, Y. Tada, T. Yokogawa, Mi. Higuchi-Takeuchi, K. Hanada, M. Matsui, Y. Ikeda, Y. Hojo, T. Hirayama, K. Kusunoki, H. Koyama, N. Mitsuda, and Y. Y. Yamamoto. 2019. "Transcriptome analysis and identification of a transcriptional regulatory network in the response to H_2O_2." Plant Physiology 180(3): 1629-1646. doi:10.1104/pp.18.01426.

Ho, C. H., S. H. Lin, H. C. Hu, and Y. F. Tsay. 2009. “CHL1 functions as a nitrate sensor in plants.” Cell 138 (6): 1184-1194. doi:10.1016/j.cell.2009.07.004.

462

463 Hooper, C. M., I. R. Castleden, S. K. Tanz, N. Aryamanesh, and A. H. Millar. 2017. "SUBA4:
464 the interactive data analysis centre for Arabidopsis subcellular protein locations." Nucleic Acids
465 Research 45(D1): D1064-D1074. doi:10.1093/nar/gkw1041.

466

467 Ito, T., R. Motohashi, T. Kuromori, S. Mizukado, T. Sakurai, H. Kanahara, M. Seki, and K.
468 Shinozaki. 2002. "A new resource of locally transposed dissociation elements for screening
469 gene-knockout lines in silico on the Arabidopsis genome." Plant Physiology 129 (4): 1695-1699.
470 doi:10.1104/pp.002774.

471

472 Jian, S., Q. Liao, H. Song, Q. Liu, J. E. Lepo, C. Guan, J. Zhang, A. M. Ismail, and Z. Zhang.
473 2018. "NRT1.1-related NH_4^+ toxicity is associated with a disturbed balance between NH4+
474 uptake and assimilation." Plant Physiology 178(4): 1473-1488. doi:10.1104/pp.18.00410.

475

476 Krouk, G., B. Lacombe, A. Bielach, F. Perrine-Walker, K. Malinska, E. Mounier, K. Hoyerova,
477 P. Tillard, S. Leon, K. Ljung, E. Zazimalova, E. Benkova, P. Nacry, and A. Gojon. 2010.
478 "Nitrate-regulated auxin transport by NRT1.1 defines a mechanism for nutrient sensing in
479 plants." Developmental Cell 18(6): 927-937. doi:10.1016/j.devcel.2010.05.008.

480

481 Krouk, G., C. Carré, C. Fizames, A. Gojon, S. Ruffel, and B. Lacombe. 2015. "GeneCloud
482 reveals semantic enrichment in lists of gene descriptions." Molecular Plant 8 (6): 971-973. doi:
483 10.1016/j.molp.2015.02.005.

484

485 Kuromori, T., T. Hirayama, Y. Kiyosue, H. Takabe, S. Mizukado, T. Sakurai, K. Akiyama, A.
486 Kamiya, T. Ito, and K. Shinozaki. 2004. "A collection of 11800 single-copy Ds transposon
487 insertion lines in Arabidopsis." The Plant Journal 37(6): 897-905. doi:
488 10.1111/j.1365.313x.2004.02009.x.

489

490 Lager, I. D. A., O. L. A. Andréasson, T. L. Dunbar, E. Andreasson, M. A. Escobar, and A. G.
491 Rasmusson. 2010. "Changes in external pH rapidly alter plant gene expression and modulate
492 auxin and elicitor responses." Plant, Cell & Environment 33(9): 1513-1528.
493 doi:10.1111/j.1365-3040.2010.02161.x.

494

495 Li, G., L. Zhang, M. Wang, D. Di, H. J. Kronzucker, and W. Shi. 2019. "The Arabidopsis
496 *AMOT1/EIN3* gene plays an important role in the amelioration of ammonium toxicity." Journal
497 of Experimental Botany 70(4): 1375-1388. doi:/10.1093/jxb/ery457.

498

499 Liu, K. H., Y. Niu, M. Konishi, Y. Wu, H. Du, H. S. Chung, L. Li, M. Boudsocq, M.
500 McCormack, S. Maekawa, T. Ishida, C. Zhang, K. Shokat, S. Yanagisawa, and J. Sheen. 2017.
501 "Discovery of nitrate-CPK-NLP signalling in central nutrient-growth networks." Nature 545:
502 311-316. doi:10.1038/nature22077.

503

504 Liu, X. X., Y. X. Zhu, X. Z. Fang, J. Y. Ye, W. X. Du, Q. Y. Zhu, X. Y. Lin, and C. W. Jin.
505 2020. "Ammonium aggravates salt stress in plants by entrapping them in a chloride

over-accumulation state in an NRT1.1-dependent manner." Science of The Total Environment 746: 141244. doi:10.1016/j.scitotenv.2020.141244.

Liu, K. H., M. Liu, Z. Lin, Z. F. Wang, B. Chen, C. Liu, A. Guo, M. Konishi, S. Yanagisawa, G. Wanger, and J. Sheen. (2022). "NIN-like protein 7 transcription factor is a plant nitrate sensor." Science, 377(6613), 1419-1425. doi: 10.1126/science.add1104.

Mounier, E., M. Pervent, K. Ljung, A. Gojon, and P. Nacry. 2014. "Auxin-mediated nitrate signalling by NRT1.1 participates in the adaptive response of *Arabidopsis* root architecture to the spatial heterogeneity of nitrate availability." Plant, Cell and Environment 37(1): 162-174. doi:10.1111/pce.12143.

Okamoto, Y., T. Suzuki, D. Sugiura, T. Kiba, H. Sakakibara, and T. Hachiya. 2019. "Shoot nitrate underlies a perception of nitrogen satiety to trigger local and systemic signaling cascades in Arabidopsis thaliana." Soil Science and Plant Nutrition 65 (1): 56-64. doi:10.1080/00380768.2018.1537643.

Patterson, K., T. Cakmak, A. Cooper, I. D. A. Lager, A. G. Rasmusson, and M. A. Escobar. 2010. "Distinct signalling pathways and transcriptome response signatures differentiate ammonium- and nitrate-supplied plants." Plant, cell & environment 33(9): 1486-1501. doi:10.1111/j.1365-3040.2010.02158.x.

528 Podgorska, A., M. Ostaszewska, P. Gardeström, A. G. Rasmusson, and B. Szal. 2015. "In
529 comparison with nitrate nutrition, ammonium nutrition increases growth of the frostbite1 A
530 rabidopsis mutant." Plant, Cell and Environment 38(1): 224-237. doi:10.1111/pce.12404.
531
532 Podgórska, A., M. Burian, K. Gieczewska, M. Ostaszewska-Bugajska, J. Zebrowski, D. Solecka,
533 and B. Szal. 2017. "Altered cell wall plasticity can restrict plant growth under ammonium
534 nutrition." Frontiers in Plant Science 8: 1344. doi:10.3389/fpls.2017.01344.
535
536 Remans, T., P. Nacry, M. Pervent, S. Filleur, E. Diatloff, E. Mounier, P. Tillard, B. G. Forde,
537 and A. Gojon. 2006. "The Arabidopsis NRT1.1 transporter participates in the signaling pathway
538 triggering root colonization of nitrate-rich patches." Proceedings of the National Academy of
539 Sciences of the United States of America 103 (50): 19206-19211.
540 doi:10.1073/pnas.0605275103.
541
542 Riveras, E., J. M. Alvarez, E. A. Vidal, C. Oses, A. Vega, and R. A. Gutiérrez. 2015. "The
543 calcium ion is a second messenger in the nitrate signaling pathway of Arabidopsis." Plant
544 Physiology 169 (2): 1397-1404. doi:10.1104/pp.15.00961.
545
546 Shen, X., Z. Wang, X. Song, J. Xu, C. Jiang, Y. Zhao, C. Ma, and H. Zhang. 2014.
547 "Transcriptomic profiling revealed an important role of cell wall remodeling and ethylene
548 signaling pathway during salt acclimation in Arabidopsis." Plant Molecular Biology 86:
549 303-317. doi:10.1007/s11103-014-0230-9.

550

551 Tsay, Y. F., J. I. Schroeder, K. A. Feldmann, and N. M. Crawford. 1993a. "The herbicide
552 sensitivity gene *CHL1* of Arabidopsis encodes a nitrate-inducible nitrate transporter." Cell 72
553 (5): 705-713. doi:10.1016/0092-8674(93)90399-B.

554

555 Tsay, Y. F., M. J. Frank, T. Page, C. Dean, and N. M. Crawford. (1993b) Identification of a
556 mobile endogenous transposon in *Arabidopsis thaliana*. Science 260 (5106): 342-344. doi:
557 10.1126/science.838580.

558

559 Vidal, E. A., V. Araus, C. Lu, G. Parry, P. J. Green, G. M. Coruzzi, and R. A. Gutiérrez. 2010.
560 Nitrate-responsive miR393/AFB3 regulatory module controls root system architecture in
561 *Arabidopsis thaliana*. Proceedings of the National Academy of Sciences. 107 (9): 4477-4482.
562 doi:10.1073/pnas.0909571107.

563

564 Walch-Liu, P., and B. G. Forde. 2008. "Nitrate signalling mediated by the NRT1.1 nitrate
565 transporter antagonises L-glutamate-induced changes in root architecture." The Plant Journal
566 54(5): 820-828. doi:10.1111/j.1365-313X.2008.03443.x.

567

568 Wang, R., R. Tischner, R. A. Gutiérrez, M. Hoffman, X. Xing, M. Chen, G. Coruzzi, and N. M.
569 Crawford. 2004. “Genomic analysis of the nitrate response using a nitrate reductase-null mutant
570 of Arabidopsis.” Plant Physiology 136 (1): 2512-2522. doi:10.1104/pp.104.044610.

571

572 Wang, W., B. Hu, A. Li, and C. Chu. 2020. "NRT1.1s in plants: functions beyond nitrate
573 transport." Journal of Experimental Botany 71(15): 4373-4379. doi:10.1093/jxb/erz554.
574
575 Xiao, C., D. Sun, B. Liu, X. Fang, P. Li, Y. Jiang, M. He, J. Li, S. Luan, and He, K. 2022.
576 "Nitrate transporter NRT1.1 and anion channel SLAH3 form a functional unit to regulate
577 nitrate-dependent alleviation of ammonium toxicity." Journal of Integrative Plant Biology
578 64(4): 942-957. doi:10.1111/jipb.13239.
579
580 Ye, J. Y., W. H. Tian, M. Zhou, Q. Y. Zhu, W. X. Du, Y. X. Zhu, X. X. Liu, X. Y. Lin, S. J.
581 Zheng, and C. W. Jin. 2021. "STOP1 activates NRT1.1-mediated nitrate uptake to create a
582 favorable rhizospheric pH for plant adaptation to acidity." The Plant Cell 33(12): 3658-3674.
583 doi:10.1093/plcell/koab226.
584
585 Zhang, X., Y. Cui, M. Yu, B. Su, W. Gong, F. E. Balu¡ka, G. Komis, J. Šamaj, X. Shan, J. Lin.
586 2019. Phosphorylation-mediated dynamics of nitrate transceptor NRT1.1 regulate auxin flux
587 and nitrate signaling in lateral root growth. Plant Physiology 181 (2): 480-498.
588 doi:10.1104/pp.19.00346.
589
590 Zhou, Y., B. Zhou, L. Pache, M. Chang, A. H. Khodabakhshi, O. Tanaseichuk, C. Benner, and
591 S. K. Chanda. 2019. "Metascape provides a biologist-oriented resource for the analysis of
592 systems-level datasets." Nature Communications 10(1): 1523.
593 doi:10.1038/s41467-019-09234-6.

594 **Figure legends**

595 **Figure 1.** Plasma membrane-targeted NRT1.1 reduces ammonium tolerance almost
596 regardless of its phosphorylating status. (a, b) Fresh weights (FWs) of shoots from
597 11-day-old Col, *chl1-5*, *nrt1.1*, L*er*, *chl1-6*, Nossen, and *pst16286* plants grown under
598 10 mM ammonium (a) or 10 mM nitrate (b) conditions (Mean ± SD; n = 5-10). (c, d)
599 Shoot FWs in Col and NRT1.1-mCherry (eNRT1.1) lines under the control of the
600 β-estradiol-inducible promoter in the *chl1-5* background (Mean ± SD; n = 15). In one
601 dish, five seedlings of each line grown under the 10 mM nitrate condition for 5 days
602 were transferred to the 10 mM ammonium (c) or 10 mM nitrate (d) condition in the
603 absence (ethanol as a mock) or presence of 1 μM β-estradiol and further grown for 6
604 days. (e, f) Shoot FWs (e) and a representative photograph (f) from 11-day-old Col,
605 *chl1-5*, *chl1-9* (*P492L*), *T101D*, and *T101A* plants grown under 10 mM ammonium
606 conditions (Mean ± SD; n = 5). The scale bar represents 5 mm. Twelve shoots from one
607 plate were regarded as a single biological replicate. (g) The chlorophyll (*a* + *b*)
608 concentrations of shoots from 5-day-old Col, *chl1-5*, *chl1-9*, *T101D*, and *T101A*
609 seedlings grown under 10 mM ammonium (Mean ± SD; n = 3). Thirty-seven shoots
610 from one plate were regarded as a single biological replicate. (h, i) FWs of shoots from
611 11-day-old Col and *cipk23-4* plants grown under 10 mM ammonium (h) or 10 mM
612 nitrate (i) conditions (Mean ± SD; n = 5-10). (j) FWs of 3-day-old Col and *chl1-5*
613 seedlings grown under 10 mM ammonium (Mean ± SD; n = 4). (k) FWs of shoots and
614 roots from 5-, 8-, or 11-day-old Col and *chl1-5* grown under 10 mM ammonium (Mean
615 ± SD; n = 5). (l) Representative photographs of 3-day-old Col and *chl1-5* seedlings

616 grown under 10 mM ammonium and representative photographs of the adaxial side of
617 cotyledons from 5-day-old Col and *chl1-5* seedlings grown under 10 mM ammonium.
618 The scale bars represent 1 mm (3-day) and 500 μm (5-day). (a, b, h–k) Six shoots or
619 roots from one plate were regarded as a single biological replicate. In one dish, six seeds
620 of each line of wild-type and mutant were placed and grown. *$P < 0.05$; **$P < 0.01$;
621 ***$P < 0.001$ (unpaired two-tailed Welch's *t*-test). NS denotes not significant. Different
622 lowercase letters indicate significant differences evaluated by the Tukey–Kramer
623 multiple comparison test conducted at a significance level of $P < 0.05$.
624
625 **Figure 2.** NRT1.1 is expressed in various tissues under ammonium conditions. (a)
626 Relative transcript levels of *NRT1.1* in 3-day-old Col seedlings grown under 10 mM
627 ammonium or 10 mM nitrate conditions (Mean ± SD; n = 3). 45 seedlings from one
628 plate were regarded as a single biological replicate. (b) Relative transcript levels of
629 *NRT1.1* in shoots and roots from 5-, 8-, or 11-day-old Col grown under 10 mM
630 ammonium or 10 mM nitrate conditions (Mean ± SD; n = 3). 12 shoots and 12 roots
631 from one plate were regarded as a single biological replicate. (c–j) Signals of
632 NRT1.1-GFPloop from pavement cells of cotyledons from 3-day-old plants (c),
633 epidermal cells of hypocotyl from 3-day-old plants (d), mesophyll protoplasts from
634 8-day-old plants (e), epidermal and cortex cells of the primary root from 5-day-old
635 plants (f, g), primary root tip from 5-day-old plants (h), and pavement cells of
636 cotyledons from 12-day-old plants (i: horizontal central section of the cell, j: horizontal
637 section below the cell surface layer). The scale bars represent 10 μm (c, e–j) and 30 μm

638 (d). The purple signals represent autofluorescence (e) and PI fluorescence (f). The
639 images were processed by Image J version 1.53c. Figure 2h was generated by the
640 maximum intensity projection.
641

642 **Figure 3.** Genome-wide transcriptional responses caused by *NRT1.1* deficiency. (a)
643 Venn diagram showing the number of genes upregulated and downregulated in the 3-
644 and 5-day-old *NRT1.1*-deficient mutants (*chl1-5*, *nrt1.1*) compared with Col grown
645 under 10 mM ammonium. The transcripts whose expression was at least 1.5-fold
646 (3-day) or 2-fold (5-day) higher or at most 1/1.5 (3-day) or 1/2 lower (5-day) in both
647 mutants relative to that in Col were counted. The gene lists are shown in Supplementary
648 Tables S2, 3. (b) Outputs derived from GeneCloud analysis of genes upregulated and
649 downregulated in the 3-day-old *NRT1.1*-deficient mutants (*chl1-5*, *nrt1.1*) compared
650 with Col grown under 10 mM ammonium. The numbers next to the term denote the
651 number of genes containing the term and the fold enrichment. (c, d) Outputs derived
652 from Metascape analysis of genes upregulated (c) and downregulated (d) in the
653 3-day-old *NRT1.1*-deficient mutants (*chl1-5*, *nrt1.1*) compared with Col grown under 10
654 mM ammonium.

655

656 **Figure 4.** NRT1.1 primarily alters the expression of aliphatic glucosinolate biosynthesis
657 genes, ACC-responsive genes, and low pH-responsive genes under ammonium
658 conditions. (a–f) Comparisons of the expression of biosynthesis genes for aliphatic

659 glucosinolate (AGSL) and indole glucosinolate (IGSL) (a), genes upregulated and
660 downregulated by ACC application (b), genes upregulated and downregulated by NaCl
661 stress (c), genes upregulated and downregulated by H_2O_2 application (d), genes
662 upregulated and downregulated by IAA application (e), and genes upregulated and
663 downregulated by low pH treatment (f) between Col and *NRT1.1*-deficient mutants
664 (*chl1-5*, *nrt1.1*) grown under 10 mM ammonium. One hundred thirty-five seedlings
665 (3-day) from three plates and 74 seedlings (5-day) from two plates were regarded as a
666 single biological replicate. Changes in gene expression levels between Col and *chl1-5*
667 and Col and *nrt1.1* were represented as logarithms to base 2 of ratios in signal
668 intensities. *$P < 0.05$; **$P < 0.01$; ***$P < 0.001$ (two-tailed ratio paired *t*-test).

Figure 1

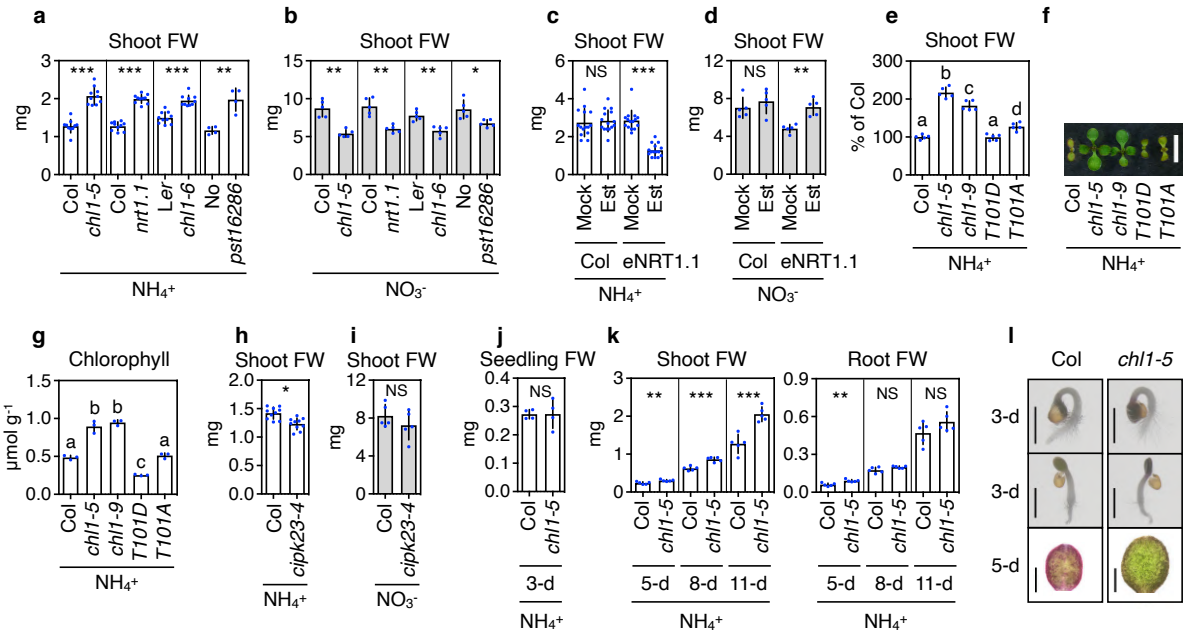
a
Shoot FW
mg
Col
chl1-5
nrt1.1
Ler
chl1-6
No
pst16286
NH4+
b
Shoot FW
NO3-
c
Shoot FW
NS
Mock
Est
Col
eNRT1.1
d
Shoot FW
e
Shoot FW
% of Col
chl1-9
T101D
T101A
f
g
Chlorophyll
µmol g-1
h
i
cipk23-4
j
Seedling FW
3-d
k
Root FW
5-d
8-d
11-d
l
Col
chl1-5

Figure 2

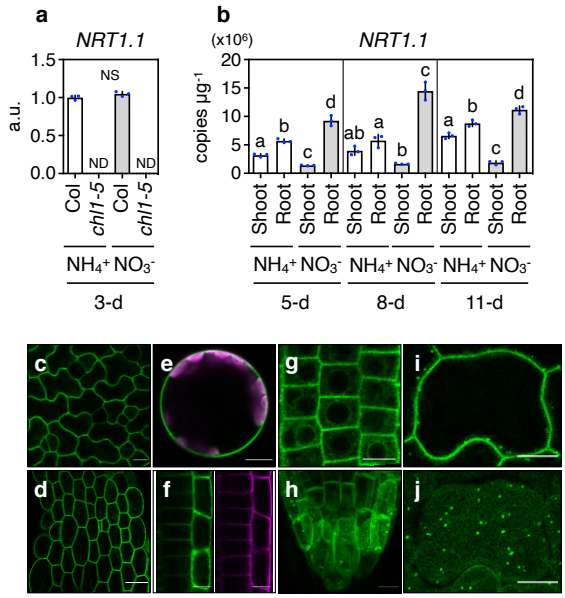
a
NRT1.1
a.u.
1.5
1.0
0.5
0.0
NS
ND
ND
Col
chl1-5
Col
chl1-5
NH4+ NO3-
3-d
b
(x10^6)
NRT1.1
copies µg-1
20
15
10
5
0
a
b
c
d
ab
a
b
c
a
b
c
d
Shoot
Root
Shoot
Root
Shoot
Root
Shoot
Root
Shoot
Root
Shoot
Root
NH4+ NO3-
NH4+ NO3-
NH4+ NO3-
5-d
8-d
11-d
c
e
g
i
d
f
h
j

Figure 3

a

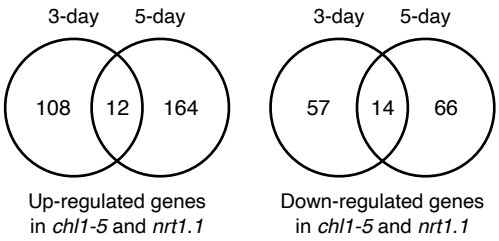

b

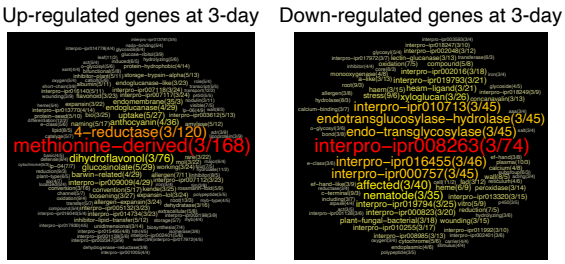

c

GO Biological Processes/KEGG Pathway/WikiPathways for Up-regulated genes at 3-day

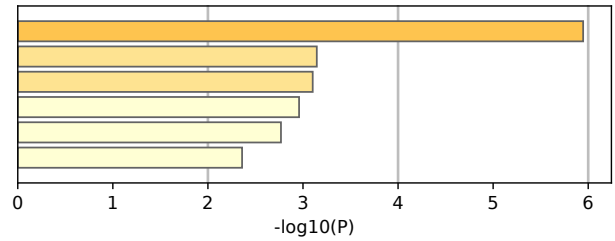

WP4597: Glucosinolate biosynthesis from methionine
GO:0009682: induced systemic resistance
GO:0009812: flavonoid metabolic process
GO:0009828: plant-type cell wall loosening
ath00910: Nitrogen metabolism - Arabidopsis thaliana (thale cress)
GO:0051049: regulation of transport

GO Cellular Components for Up-regulated genes at 3-day

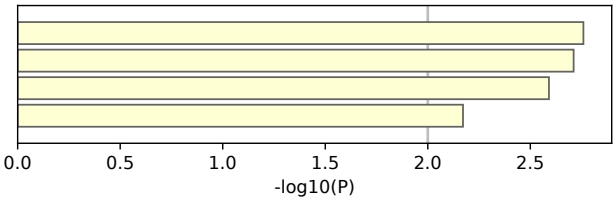

GO:0019867: outer membrane
GO:0009707: chloroplast outer membrane
GO:0099503: secretory vesicle
GO:0048046: apoplast

GO Molecular Functions for Up-regulated genes at 3-day

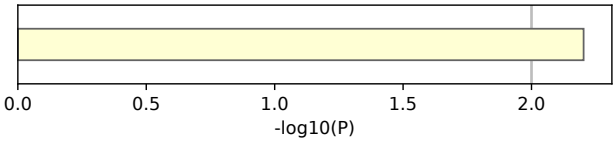

GO:0016836: hydro-lyase activity

d

GO Biological Processes/KEGG Pathway/WikiPathways for Down-regulated genes at 3-day

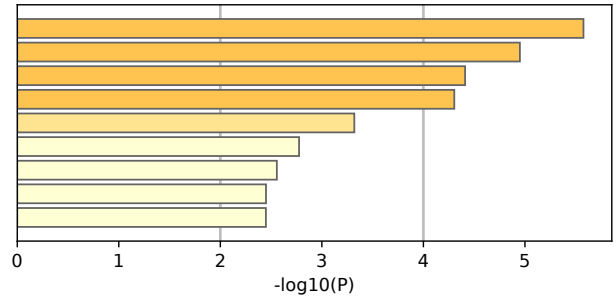

GO:0009651: response to salt stress
GO:0071456: cellular response to hypoxia
GO:0014070: response to organic cyclic compound
GO:0010200: response to chitin
GO:0010411: xyloglucan metabolic process
GO:0006979: response to oxidative stress
ath04146: Peroxisome - Arabidopsis thaliana (thale cress)
GO:0071369: cellular response to ethylene stimulus
GO:0009409: response to cold

GO Cellular Components for Down-regulated genes at 3-day

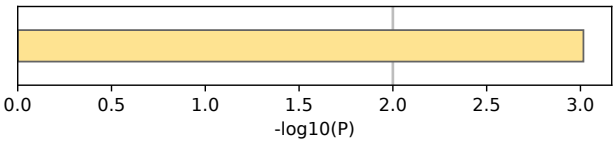

GO:0009505: plant-type cell wall

GO Molecular Functions for Down-regulated genes at 3-day

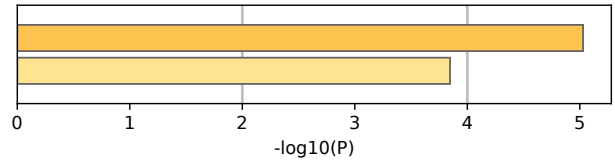

GO:0016209: antioxidant activity
GO:0016762: xyloglucan:xyloglucosyl transferase activity

Figure 4

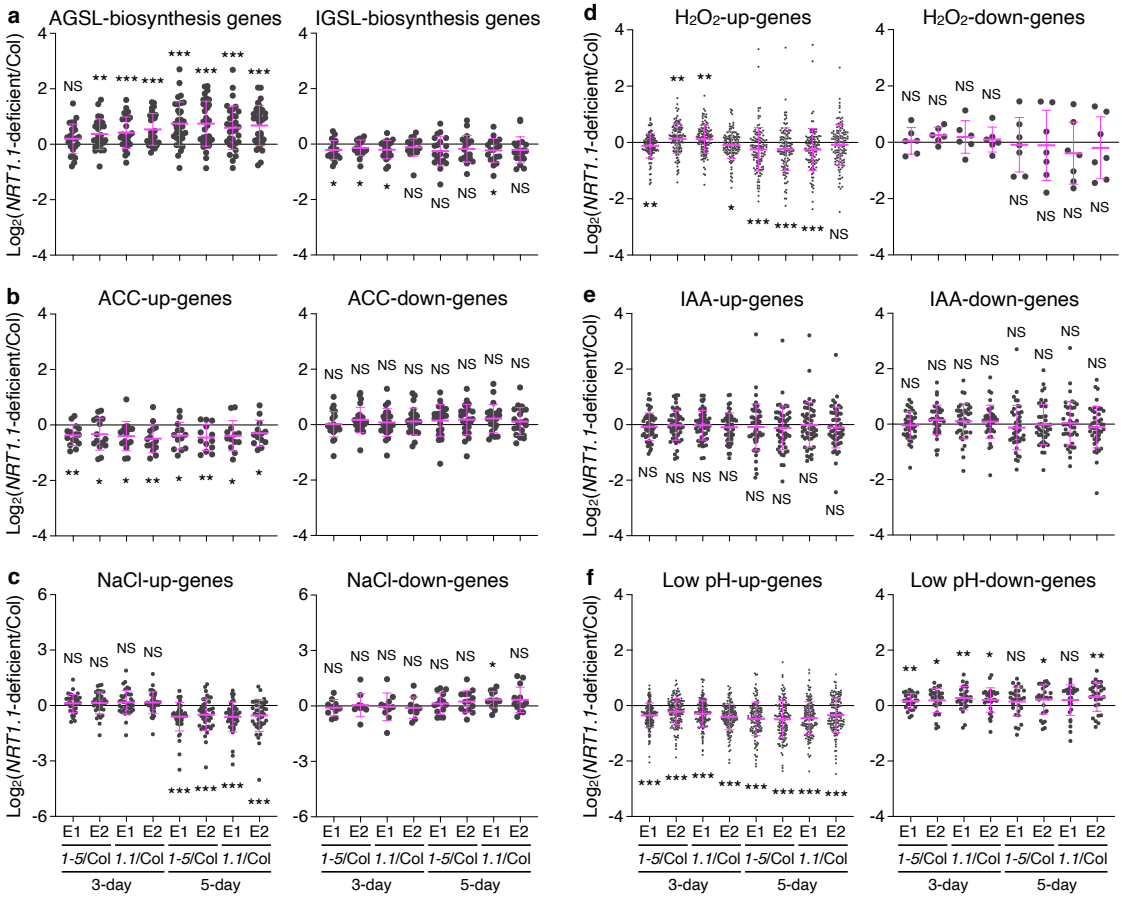
a
AGSL-biosynthesis genes
IGSL-biosynthesis genes
b
ACC-up-genes
ACC-down-genes
c
NaCl-up-genes
NaCl-down-genes
d
H2O2-up-genes
H2O2-down-genes
e
IAA-up-genes
IAA-down-genes
f
Low pH-up-genes
Low pH-down-genes
Log2(NRT1.1-deficient/Col)
E1 E2 E1 E2 E1 E2 E1 E2
1-5/Col 1.1/Col 1-5/Col 1.1/Col
3-day
5-day